MEASUREMENT OF PLASMA WAVE SPEED FROM ELECTRON BEAM END EROSION*

D. F. Sutter and B.L. Beaudoin, Institute for Research in Electronics and Applied Physics, University of Maryland, College Park, MD 20742, USA

Abstract

The University of Maryland Electron Ring (UMER) normally injects a beam that is square in longitudinal profile (constant line density), filling one half the ring. When operating without longitudinal focusing, the beam head and tail erode at a constant plasma wave speed. Because the beam is very long (580 cm) compared to the beam pipe diameter (5 cm), the two eroding edges remain sharply defined until they meet. This paper describes how the plasma wave speed in the beam can be obtained experimentally by measuring only the initial pulse length, the time it takes for the eroding ends to meet and the kinetic energy. The plasma wave velocity can then be used to get an estimate of the average beam radius during the erosion time. Experimental results are compared to theoretical predictions.

INTRODUCTION

The University of Maryland Electron Ring (UMER) was built to explore the physics of non relativistic, space charge dominated beams that would be relevant for an ion accumulator ring of the type originally envisaged for application in heavy ion fusion. While the operating kinetic energy of 10 keV is very low, it is sufficient at the range of available operating currents, 0.6 to 100 mA, to serve as a good analog model for such accumulator rings. Moreover, because the relativistic gamma factor is only 1.02, there also exist a whole range of non neutral plasma phenomena that cannot be so easily observed in a highly relativistic beam. One of these is the ready generation and observation of plasma density waves. In UMER the beam can be operated with or with out longitudinal confinement [1]. When there is no longitudinal confinement, the initially almost square ends of the injected pulse begin to immediately disperse, or "erode" in a characteristic debunching pattern as shown in Figure 1. The electrons at the leading edge are pushed forward, gaining kinetic energy from the potential energy stored in the electrical potential of the beam charge, and electrons at the trailing edge are decelerated, in effect losing kinetic energy. The edges where the beam is actively eroding into the constant line charge density in the longitudinal beam center retain a sharp definition up to the point where the two edges come together in what is called the "breakpoint" in Figure 1. The rate at which each edge moves toward the center is the plasma wave velocity, c_s, and that is what is measured in this experiment.

PHYSICS OF THE EXPERIMENT

Boundary Conditions

The general operating parameters of UMER have been described elsewhere [2] as has the generation of density waves and solitons [3][4][5][6]. The specific properties that support the non neutral plasma experiments and modelling with cold fluid equations for space charge dominated beams are, the very long bunch length compared to the beam pipe diameter, the low beam velocity, the presence of strong space charge (for beam currents > 1 mA), and a beam density that is approximately constant over the radius. As a consequence, the radial component of the electric field, E_r, points outward and $E_z = 0$ in the region between the eroding edges. In the region between an eroding edge and the head or tail end point, E_z is proportional to the gradient in z of the line charge density, which is no longer constant. Of particular importance to the present technique, the 10 keV beam injected into UMER has an almost rectangular, constant initial line charge density profile with rise and fall times of a few nanoseconds, and a flat top of adjustable pulse length (~20 to 145 ns).

Computing the Wave velocity

The wave velocity, usually referred to as the "sound velocity" of the density wave because it is analogous to the ion acoustic velocity in neutral plasma, can be computed from [4],

$$c_s = \sqrt{\frac{e}{4\pi\varepsilon_0}\frac{1}{m_0 v_{bm}}\frac{g}{\gamma^5}I_{bm}} \quad , \text{ where } \quad g = 2\ln\frac{b}{a} \qquad (1)$$

for space charge dominated beams [3]. Noting that the classical radius of the electron r_e and the "characteristic current" I_0 are defined, respectively, by

$$r_e = \frac{e^2}{4\pi\varepsilon_0 m_0 c^2} \text{ and } \quad I_0 = \frac{e\,c}{r_e},$$

Equation (1) can be rewritten in a more convenient form as

$$c_s = c\sqrt{\frac{1}{\beta\gamma^5}\frac{I_{bm}}{I_0}2\ln\frac{b}{a}} \,, \qquad (2)$$

where c is the velocity of light, β and γ are the usual relativistic parameters, b is the beam pipe inner diameter and a is the beam radius. Given a set of beam radii corresponding to the relevant operating parameters,
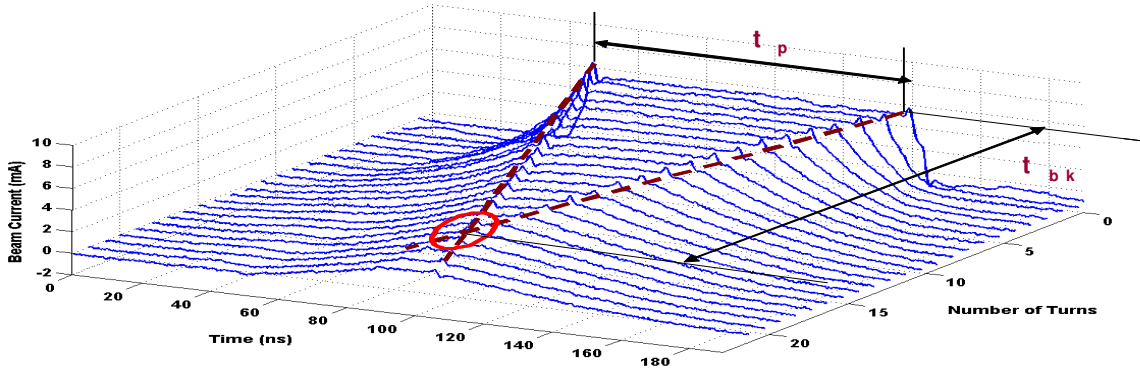
Figure 1: Mountain top plot of UMER 6 mA beam debunching past the "Break Point."

including the emittance at injection, and beam currents, equation (2) is used to compute the set of predicted values of c_s, shown in Table 1, column 3, corresponding to the initial beam radii shown in column 6. Solving equation (2) for the beam radius,

$$a = b\, e^{-A\frac{c_s^2}{I_{bm}}} \text{ , with } A = \frac{\beta\gamma^5 I_0}{2c^2} \qquad (3)$$

Equation (3) can then be used to compute a value of average beam radius based on the independent measurement of c_s described in the following section.

Sound Speed from Times

If the length of a beam pulse is t_p, and the velocity of the 10 keV beam is v_{bm}, the beam has a physical length $l = v_{bm}t_p$. But since the two edges are moving towards each other at the sound speed c_s, the edges will cover the same distance l in $2c_s t_{bk}$, where t_{bk} is the break point time that it takes the two edges to come together. Since the distance is the same, $v_{bm}t_p = 2c_s t_{bk}$ and

$$c_s = \frac{1}{2} v_{bm} \frac{t_p}{t_{bk}} \qquad (4)$$

So to measure the sound speed, it is only necessary to know three quantities: kinetic energy (to get v_{bm}) and the two times, the initial pulse length and the time to breakpoint. To compute the average beam radius for a measured c_s using equation (3), the corresponding beam current must also be measured.
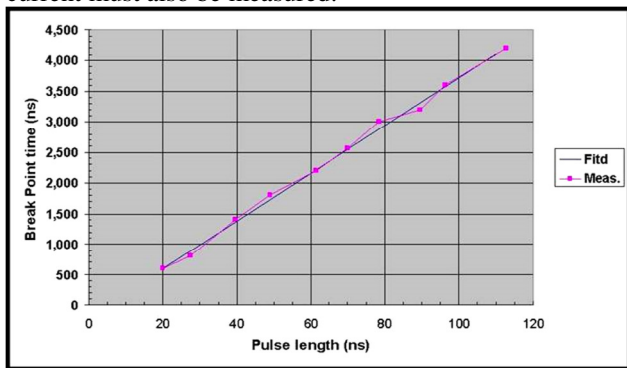
Figure 2: A plot of the measured values of t_{bk} vs t_p for a 6.0 mA beam.

MEASUREMENTS

In order to get a more accurate determination of the sound speed, t_{bk} was measured over a range of pulse lengths, and this was done for three different beam currents, I_{bm} = 0.6, 6.0 and 20.0 mA. The injected beam current is measured using a calibrated Bergoz integrating current monitor in the injection line and the values t_p and t_{bk} from a wall current monitor in the ring that displays the circulating beam current on a Tektronix DPO7254 oscilloscope. A plot of a typical data set is shown for the 6.0 mA beam in Figure 2. A linear fit is then made to the data which gives the slope and related errors as standard deviations. The fit also defines a linear relation

$$t_{bk} = mt_p + d \text{ ,}$$

where m is the slope and d the offset at $t_p = 0$, that can be used to predict t_{bk}. Using equation (4), the measured value of c_s in column 2 of Table 1 is computed from

$$c_s = \frac{1}{2}\frac{v_{bm}}{m}, \text{ where } m = \left\langle \frac{t_{bk}}{t_p} \right\rangle_{fit}. \qquad (5)$$

Each of the measured values of c_s is an average over the time t_{bk}; so equation (5) gives a sort of "average of averages" of c_s over the t_{bk} versus t_p data sets.

All of the measurements were made with a beam kinetic energy of 10.000 keV giving a value of v_{bm} = 5.846 cm/ns, calculated from the special relativity relation for v_{bm} as a function of kinetic energy and electron rest energy. This was done to avoid a systematic error of ~ 1.4 % that would occur by using the nonrelativistic relation. The systematic error in equation (5) is calculated from,

$$\Delta c_s = \frac{1}{2m}\left(\Delta v_{bm} - \frac{v_{bm}}{m}\Delta m \right); \qquad (6)$$

Δm is the standard deviation of m obtained from the linear fitting routine. The results for three beam currents are shown in Table 1.

Table 1: Results of measuring the sound speed in the core of the UMER beam for several beam currents. The predicted radii in column 6 are based on the computed emittance of the beam generated at the exit of the electron gun [7]. These emittances have been confirmed by independent measurements using tomographic techniques [8]. The predicted radii are used to compute the predicted c_s values in column 3.

Beam Current (mA)	Meas. c_s (cm/ns)	Pred. c_s (cm/ns)	Percent Difference	Est. Beam Radius(mm)	Pred. Beam Radius (mm)	Percent Diff.
0.58	0.0274 ± 0.0002	0.0276	0.7	1.78 ± 0.01	1.71	4.0
6.0	0.0750 ± 0.0015	0.0752	0.3	3.69 ± 0.04	3.64	1.4
20.5	0.1282 ± 0.0040	0.1223	3.5	4.87 ± 0.34	5.64	13.6

The average beam radii in column 5 of Table 1 are computed from equations (3). The contribution to the error in the exponential is dominated by the errors from values for c_s and I_{bm}; so the much smaller error in A is ignored in the following expression for the error in measured beam radius,

$$\Delta a = \left\{ \frac{\Delta b}{b} - \left[2\frac{c_s}{I_{bm}}\Delta c_s - \left(\frac{c_s}{I_{bm}}\right)^2 \Delta I_{bm} \right] A \right\} a \quad (7)$$

We have used the following values in calculating the entries in table 1: b= 24.89 ± 0.089 mm, ΔI_{bm} = ± 0.2 mA for all beam currents and v_{bm} = 5.846 ± .006 cm/ns based on our best estimate for momentum spread, Δp = ± 20 eV.

CONCLUSIONS

The derivation of equation (1) for c_s using the one dimensional fluid model in the cited references assumes that the electron beam is space charge dominated. The 0.6 mA beam, although it exhibits lots of serious space charge effects, is considered emittance dominated. So using the definition of equation (1) instead of the non space charge definition,

$$g = \left(\frac{1}{2} + 2\ln\frac{b}{a} \right),$$

was a question. The results in Table 1 confirm that the space charge dominated form of g works for 0.6 mA. Based on operating experience with UMER, there have been problems of beam blow up with the 0.6 mA beam, associated with injection line quadrupole settings, over the ~50 turns required to reach t_{bk}. We have found only a few sets of injection quad settings that reduce the blow up, and the presented results confirm the effectiveness of the settings used for the measurements. The lack of significant blow up for these quad values has been confirmed by kicking the 0.6 mA beam out, turn - by – turn, onto a phosphor screen for a direct, but laborious, measurement of beam radius.

Beam loss has a variety of causes, and all of these can change the assumed constant line charge density in the flattop region of the beam pulse. There are also a variety of potential causes of emittance blow up

implying a corresponding radial size blow up. This experiment cannot distinguish among such causes, but the measured results for average c_s and a_{avg} for the 0.6 and 6.0 mA beams indicate that such effects are minimal over the corresponding times to t_{bk} (~50 turns for 0.6 mA and ~18 turns for 6.0 mA at t_p = 100 ns) and the machine operating parameters in place during the measurements. Beam and emittance blow up are known issues for the more strongly space charge dominated 20 mA beam. So the measured results are better than expected, but then the number of turns to t_{bk} is only ~10 or 11- not a very long sample of beam behaviour.

In summary, the work presented shows that the use of this simple c_s measurement technique is a quick and easy way to get an estimate of beam behaviour over the store time from injection to the breakpoint and is easier than the beam knockout and phosphor screen method that is our only other present alternative.

REFERENCES

[1] B. Beaudoin, I. Haber, R.A. Kishek, S. Bernal, T. Koeth, D. Sutter, P.G. O'Shea, and M. Reiser Physics of Plasmas **18**, 013104 (2011).

[2] R. Kishek, et al,"The University of Maryland Electron Ring Program," Proceedings, U.S. PAC 2013.

[3] K. Takayama and R. Briggs" Induction Accelerators," Springer, Berlin 2011.

[4] J.J. Deng et al, "Longitudinal Focusing of a Space-Charge Dominated Beams in the U of MD Electron Ring," U.S. PAC 1997.

[5] D.X. Wang et al, "Restoration of Rectangular Pulse Shape after Edge Erosion for a Space-Charge Dominated Electron Beam" PRL, 73, 1 (1994).

[6] Y. Mo, R.A. Kishek, D. Feldman, I. Haber, B. Beaudoin, P.G. O'Shea, and J.C.T. Thangaraj, Physical Review Letters **110**, 084802 (2012).

[7] Internal Note: UMER-09-0730-RAK.

[8] D. Stratakis, R.A. Kishek, S. Bernal, R.B. Fiorito, *et al.*, *"Generalized Phase-Space Tomography for Intense Beams,"* Physics of Plasmas **17**, 056701 (2010).